



Photoinduced electron and energy transfer from coumarin 153 to perylenetetracarboxylic diimide in bmimPF₆/TX-100/water microemulsions

Haixia Wu, Haixia Wang, Lin Xue, Xiyou Li*

Key Laboratory of Colloid and Interface Chemistry, Ministry of Education, Department of Chemistry, Shandong University, Jinan 250100, China

ARTICLE INFO

Article history:

Received 23 June 2010

Accepted 22 September 2010

Available online 29 September 2010

Keywords:

Electron transfer

Energy transfer

Coumarin 153

Perylenetetracarboxylic diimide

ABSTRACT

A perylenetetracarboxylic diimide (PDI) compound with an attached hydrophilic polyoxyethylene group at the imide nitrogen position was designed and synthesized. Photoinduced electron and energy transfer between coumarin 153 (C-153) and PDI in a ternary microemulsion with an ionic liquid (bmimPF₆/TX-100/H₂O) were investigated by steady state electronic absorption and fluorescence spectroscopy. The results revealed that both PDI and C-153 resided at the interface between the surfactant TX-100 and the ionic liquid bmimPF₆ in the ternary microemulsions. The absorption spectra suggested no interactions between C-153 and PDI in the ground states, but the fluorescence spectra revealed the presence of an efficient electron transfer and a less efficient energy transfer from C-153 to PDI. Moreover, the electron transfer was much more efficient in microemulsions than that in homogeneous conventional organic solvents due to the unique micro-environment of the microemulsion.

© 2010 Elsevier Inc. All rights reserved.

1. Introduction

Ionic liquid (IL) microemulsions have attracted much interest in theoretical and practical aspects. For example, Han and his co-workers obtained polar nanosize droplets of 1-butyl-3-methylimidazolium tetrafluoroborate (bmimBF₄) dispersed in continuous hydrocarbon solvent, which were similar in shape to “classic” water-in-oil (W/O) microemulsions [1]. Gao prepared successfully a ternary microemulsion of bmimPF₆/TX-100/water. Three types of microstructure were observed for the microemulsions, and the hydrodynamic diameter of the spherical microemulsion increased along with the increase of bmimPF₆/TX-100 ratio [2]. Chakrabarty investigated the effects of bmimBF₄ on solvation dynamics and rotational relaxation of coumarin 153 in TX-100/cyclohexane microemulsion by steady-state and time-resolved emission spectroscopy method [3]. Seth et al. revealed that the solvation time of coumarin 153 and coumarin 151 in bmimPF₆/TX-100/water microemulsion is largely dependent on the probe location in the microemulsion [4]. Li explored the micropolarities of bmimBF₄/TX-100/toluene microemulsion by using methyl orange and methylene blue as probes. The microemulsion was revealed to be good solvent for ionic salt compounds and biochemical reagents, like riboflavin [5].

IL microemulsions were also used widely as chemical reaction media, representative examples include alkylation of 2-alkylindan-1,3-diones with benzyl bromide [6], detoxification of mustard

[7], oxidation of *p*-Me₂NC₆H₄NH₂ and Fe(CN)₆⁴⁻ [8,9], synthesis of metalloporphyrin and sodium dodecyl sulfonate [10,11]. In addition, microemulsions had also been applied to enzymic reactions to enhance the stability of biocatalysts and increase the reaction rate [12,13]. Bhattacharyya and co-workers studied the energy transfer between coumarin 480 and rhodamine 6G in a IL microemulsion and found that several different energy transfer mechanisms coexist in this system due to the distribution of coumarin 480 in the different region of the IL microemulsion [14]. However, the effects of the IL microemulsion on the energy transfer and electron transfer is far from thoroughly understood yet. More research in this field is necessary.

Perylenetetracarboxylic diimides (PDIs) received great deal of attentions as photoactive materials [15–22]. They showed great potential of realistic application as organic field-effect transistors [23–25], light-harvesting solar cells [26–31], and light-emitting diodes [32–36]. Furthermore, PDI chromophores offered broad spectral coverage and large extinction coefficient in near-infrared range, therefore, they were frequently employed in single molecule spectroscopic studies [37–41] and construction of multichromophoric arrays for energy and electron-transfer studies [42,43]. Recently, energy and electron transfer involving PDIs had been investigated in organic solvents, molecular aggregates and even in solid-states [44–47]. However, studies on PDI in confined IL microemulsions were never reported so far. The unique microenvironment of the IL microemulsion is expected to affect the photoinduced energy or electron transfer reactions significantly. The fundamental understanding on the effects of IL microemulsion on the intermolecular photoinduced electron or energy transfer is

* Corresponding author. Fax: +86 (0)531 8856 4464.

E-mail address: xiyouli@sdu.edu.cn (X. Li).

very important for the design of novel artificial light harvesting systems or reaction centers with IL microemulsion as reaction media.

Herein, we report the design and synthesis of an amphiphilic PDI which can dissolve freely in a ternary IL microemulsion. The energy and electron transfer from hydrophobic coumarin 153 (C-153) to PDI in bmimPF₆/TX-100/H₂O ternary microemulsion are studied by means of UV–vis absorption and emission spectra, and compared with that in polar or non-polar organic solvents.

2. Materials and methods

2.1. Materials

The structures of C-153 and PDI are shown in Scheme 1. Table 1 presents the composition of the microemulsion. C-153 was purchased from Sigma and used as received. BmimPF₆ was prepared as reported in literature [48], which was further dried in a vacuum for 4 h at 80 °C before use. TX-100 and other chemicals were purchased from commercial source and used as received without further purification. Synthesis and characterization of PDI was described in Supporting Information. The final concentration of C-153 in all experiments was kept at 5×10^{-6} M. PDI and C-153 M ratios were 0, 0.2, 0.5, 0.8 and 1.0 in organic solvent and microemulsion. All samples were stored for ten days before different photophysical measurements.

2.2. General method

¹H NMR spectra were recorded on a Bruker DPX 300 spectrometer (300 MHz). MALDI–TOF mass spectra were recorded on a Bruker BIFLEX III mass spectrometer with cyano-4-hydroxycinnamic acid as matrix. The diameter of the microemulsion was determined by dynamic light scattering (DLS) on a DAWN HELEOS instrument with laser operating at 658 nm. Electrochemical measurements were carried out on a BAS CV-50 W voltammetric analyzer with a glassy carbon disk working electrode (2.0 mm in diameter), a silver-wire counter electrode, and an Ag/Ag⁺ reference electrode. Tetrabutylammonium perchlorate in freshly distilled CH₂Cl₂ (0.1 mol dm⁻³) was used as the electrolyte solution. Ferrocene was employed as the reference redox system according to IUPAC's recommendation [49]. Electronic absorption spectra were recorded on a Hitachi U-4100 spectrophotometer. Steady state fluorescence

spectra were recorded on ISIS K2 system (USA). The fluorescence lifetimes were measured on FLS920 system (Edinburgh Instruments). For steady-state and time-resolved emission experiments, all samples were excited at 400 nm and carried out at room temperature.

3. Results and discussion

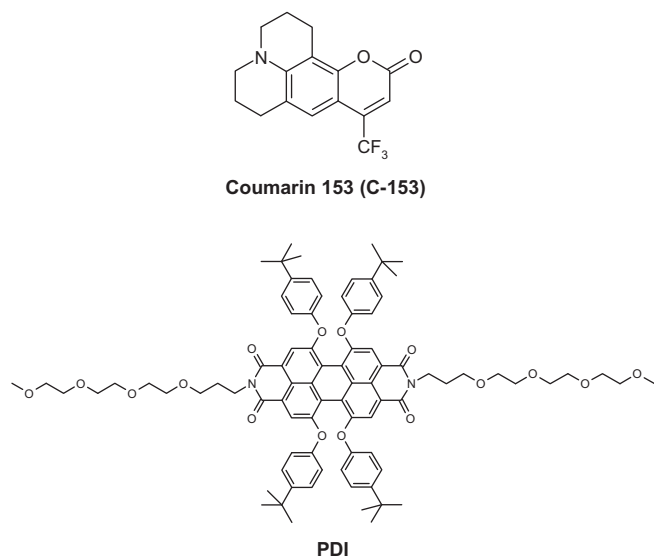
3.1. Locations of C-153 and PDI in the microemulsion

The ternary microemulsion is comprised of 1-butyl-3-methylimidazolium hexafluorophosphate (bmimPF₆), Triton X-100 (TX-100), and water. In such a heterogeneous environment, the surfactant (TX-100) molecules aggregate in form of a peripheral shell around the pool of the ionic liquid, the ethylene oxide chains of TX-100 and water form the outer layer. The polarity of the microemulsion varies from a relative low polar environment near the alkyl chains of the surfactant at the interface between IL and TX-100 to a high polar region in the core of the ionic liquid pool [4,5,14,50]. Dynamic light scattering (DLS) experiments reveal the formation of IL microemulsion with hydrodynamic diameters around 5.8 nm. The measured hydrodynamic diameter is a little bit smaller than that reported in literature [4], which maybe caused by the different experimental temperatures and/or surfactant qualities.

The absorption and emission spectra of a probe molecule are sensitive to the polarity of the environment [4,5,51]. In order to determine the location of PDI in the microemulsion, we recorded firstly the absorption and emission spectra of PDI in three pure organic solvents with different polarity. The maximal absorption band of PDI in toluene, tetrahydrofuran and bmimPF₆ centered at about 573 nm, 567 nm and 557 nm, respectively, while the corresponding emission maximum were at 604 nm, 602 nm and 590 nm. We could conclude that both absorption and emission maximum of PDI blue-shifted along with the polarity increase of the solvents.

Table 1
Composition and hydrodynamic diameter of bmimPF₆/TX-100/water microemulsion.

Water concn. (wt.%)	TX-100 concn. (wt.%)	BmimPF ₆ concn. (wt.%)	D _n (nm)
83.9	15.0	1.1	5.8



Scheme 1. Structures of C-153 and PDI.

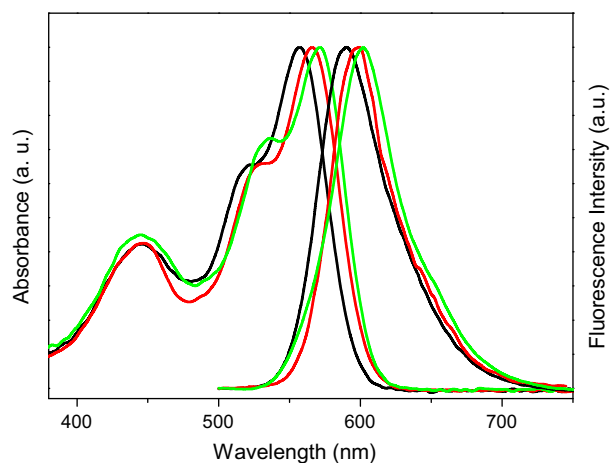


Fig. 1. Absorption and fluorescence spectra (excited at 400 nm) of PDI in bmimPF₆ (black line), 15 wt.% TX-100 solution (red line) and microemulsion (green line). (For interpretation of the references to color in this figure legend, the reader is referred to the web version of this article.)

Fig. 1 compares the absorption and fluorescence spectra of PDI in bmimPF_6 , TX-100/water mixture and microemulsion. The spectral parameters are summarized in Table 2. The maximum absorption band of PDI in 15 wt.% TX-100 aqueous solution was found at about 566 nm. On addition of IL (bmimPF_6) to the TX-100/water solution, the maximum absorption band of PDI red-shifted to 571 nm. This observation indicated directly the formation of microemulsion and the micro-environment of PDI in the microemulsion was different from that in IL solvent or TX-100/water binary system. Because the maximum absorption band of PDI in the microemulsion red-shifted significantly relative to that in TX-100/water binary system and in pure IL, most of PDI molecules in the microemulsion must reside in a less polar region, probably at the interface of TX-100 and bmimPF_6 . Similar results can be deduced from the emission spectra.

The absorption and emission maximum of C-153 in the microemulsion are at 423 and 524 nm respectively, which are consistent with the previous report [4], therefore, C-153 molecules stay at the interface of TX-100 and bmimPF_6 in the microemulsion as reported in literature. The location of C-153 and PDI in the microemulsion is schematically shown in Fig. 2.

3.2. Photoinduced energy and electron transfer from C-153 to PDI

Fig. 3 shows the absorption spectra of PDI and emission spectra of C-153 in the microemulsion. The large overlap between the absorption of PDI and emission of C-153 indicates that the photo-induced energy transfer from donor C-153 to acceptor PDI is theoretically possible in the microemulsion.

3.2.1. UV-Vis absorption spectroscopy

Fig. 4 compares the absorption spectra of C-153 and PDI with that of a 1:1 mixture of C-153/PDI in the microemulsion. The maximal absorption bands of C-153 and PDI are at 428 nm and 571 nm respectively. The absorption maximum of PDI in the 1:1 mixture does not show any shift compared to that of pure PDI. Moreover, the absorption spectra of the 1:1 mixture of PDI and C-153 are

Table 2
Absorption and emission maxima of PDI in different solvents.

	$\lambda_{\text{max}}^{\text{abs}}$ (nm)	$\lambda_{\text{max}}^{\text{flu}}$ (nm)
BmimPF_6	557	590
15 wt.% TX-100/water mixture	566	597
Microemulsion	571	602

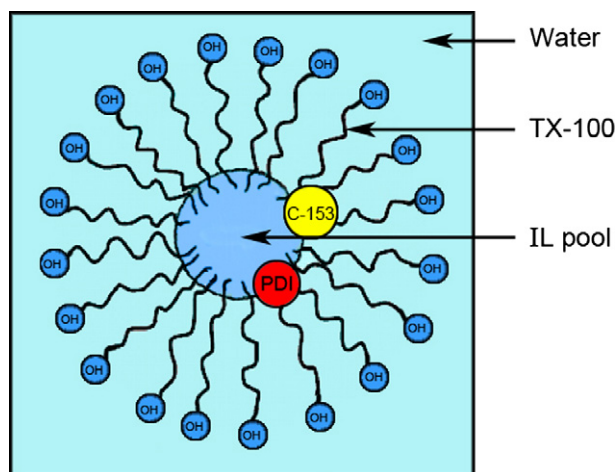


Fig. 2. Locations of C-153 and PDI in the microemulsion.

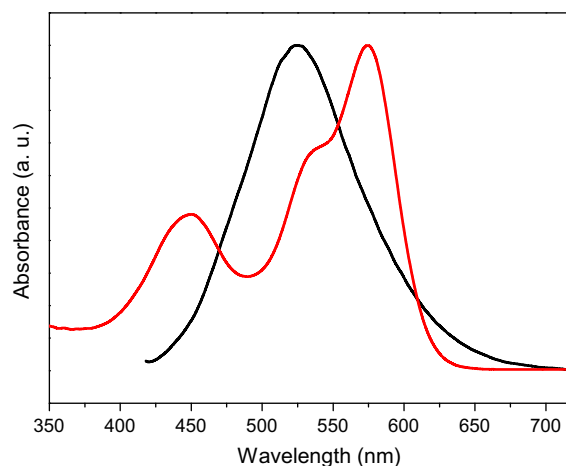


Fig. 3. Normalized absorption spectra of PDI (red line) and emission spectra of C-153 (black line) in microemulsion. (For interpretation of the references to color in this figure legend, the reader is referred to the web version of this article.)

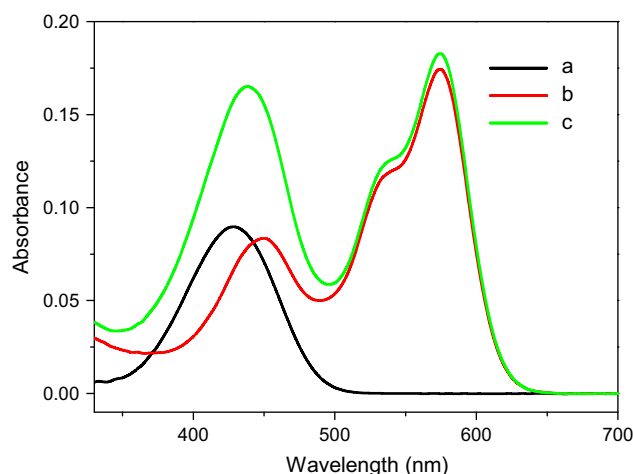


Fig. 4. Absorption spectra of C-153 (black line), PDI (red line) and a 1:1 mixture of C-153 and PDI (green line) in microemulsion (concentrations of C-153 and PDI are 5×10^{-6} M). (For interpretation of the references to color in this figure legend, the reader is referred to the web version of this article.)

almost identical to the sum of the absorption spectra of C-153 and PDI with same concentrations. All these results suggested that no interaction between C-153 and PDI at ground state in the microemulsion. Similar results have been deduced from the absorption spectra of C-153 and PDI in toluene and tetrahydrofuran (Fig. S1, Supplementary material).

3.2.2. Fluorescence spectra

Fig. 5 depicts the fluorescence spectra of the mixture of C-153 and PDI in the microemulsion with excitation at 400 nm. The emission bands centered at about 524 nm and 602 nm can be attributed to the fluorescence of C-153 and PDI, respectively. The fluorescence of C-153 is quenched gradually along with the increase on the concentration of PDI in the mixture. Both C-153 and PDI absorbs at the excitation wavelength (400 nm) with a relative absorbance ratio of 2/1 in a 1:1 mixture as calculated from the absorption spectra [52]. Therefore, the observation of the fluorescence of both C-153 and PDI in the fluorescence spectra of the mixture is reasonable because both of them are excited simultaneously. But the significant fluorescence quenching of C-153 by PDI indicates obviously the presence of one or more photoinduced processes between C-153

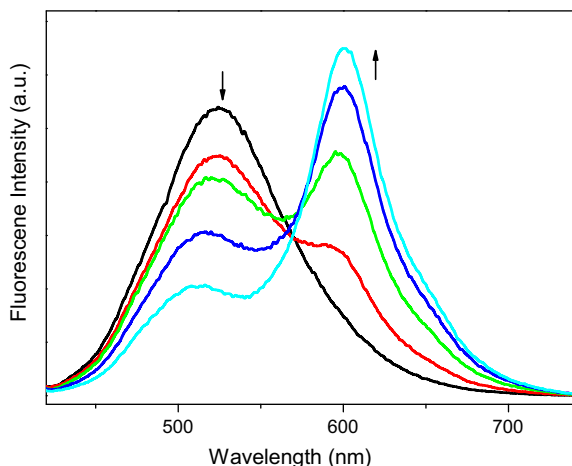


Fig. 5. Fluorescence spectra of mixture of C-153 and PDI in microemulsion, the concentration of C-153 in all samples was kept at 5×10^{-6} M, the PDI and C-153 M ratio varied from 0, 0.2, 0.5, 0.8 to 1.0.

and PDI. The fluorescence quenching efficiencies (Φ_q) are calculated by the comparison of the fluorescence intensity (I_f) of C-153 in the presence of PDI with the fluorescence intensity of C-153 without PDI (I_0) following equation:

$$\Phi_q = 1 - I_f/I_0 \quad (1)$$

The calculated results are summarized in Table 3. It can be found that the calculated Φ_q in microemulsion is significantly larger than that in toluene and THF, which indicates different fluorescence quenching mechanisms in microemulsion from that in organic solvents.

The fluorescence intensity of PDI (602 nm) increases significantly along with its concentration increase in both toluene and THF. Similar fluorescence intensity increase is also observed in microemulsion, Fig. 5. Part of this fluorescence increase can be attributed to its concentration increase. However, when the fluorescence spectra of C-153/PDI 1:1 mixture in toluene are compared with the sum of the fluorescence spectra of PDI and C-153 in toluene with the same concentration, an intensity increase for the emission of PDI and an intensity decrease for the emission of C-153 are observed simultaneously, Fig. 6. This result suggests that the fluorescence intensity increase of PDI is not totally induced by its concentration increase, but part of them is caused by singlet–singlet energy transfer from C-153 to PDI. Similar results are observed in microemulsion and THF (Figs. S3 and S4, Supplementary material).

3.2.3. Energy transfer efficiency

The energy transfer efficiency Φ_{Ent} can be calculated by comparing the number of photons received by the acceptor ($I_a(A)$) with the number of photons absorbed by the donor ($I_a(D)$) following equation:

$$\Phi_{\text{Ent}} = I_a(A)/I_a(D) \quad (2)$$

where $I_a(A)$ can be estimated from the fluorescence intensity increase of PDI caused by the energy transfer ($I_f(\text{PDI})$) and the

Table 3

Fluorescence properties of a 1:1 mixture of C-153 and PDI in different solvents.

	Φ_{Ent} (%)	Φ_q (%)	Φ_{ET} (%)
Toluene	11.4	14.0	2.6
THF	10.9	16.7	5.8
Microemulsion	2.7	61.0	58.3

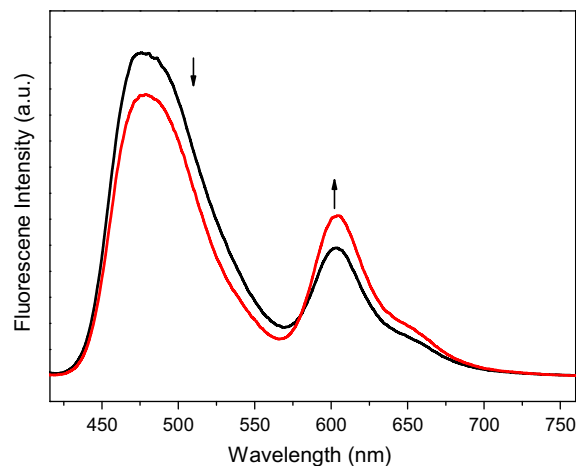


Fig. 6. Fluorescence spectra of a 1:1 mixture of C-153 and PDI (red line) and the sum of the fluorescence spectra of C-153 and PDI at same concentration (black line) in toluene with excitation at 400 nm. (For interpretation of the references to color in this figure legend, the reader is referred to the web version of this article.)

fluorescence quantum yields of PDI in the microemulsion (Φ_f) following equation:

$$I_a(A) = I_f(\text{PDI})/\Phi_f \quad (3)$$

The Φ_{Ent} from C-153 to PDI of a 1:1 mixture in different solvents are calculated and the results are summarized in Table 3. It is interesting that the calculated Φ_{Ent} are all much smaller than the corresponding Φ_q . This indicates the presence of other fluorescence quenching process between C-153 and PDI.

It is worth noting that the Φ_{Ent} in THF or toluene is much larger than that in the microemulsion while the Φ_q in THF or toluene is much smaller than that in the microemulsion. As mentioned above, both C-153 and PDI stay at the interface of IL/TX-100, they are restricted in a very small space. Therefore, the local concentrations of both PDI and C-153 at the interface between TX-100 and IL are much higher than that of the body solution, and accordingly results in a higher Φ_q . The smaller energy transfer efficiencies observed in the microemulsion may be ascribed to the competition of the second fluorescence quenching process, which has been enhanced significantly by the unique environment of the microemulsion. This will be discussed further in the following parts.

3.2.4. Electron transfer from C-153 to PDI

According to the previous reports [53–55], PDIs are good electron acceptors with low reduction potentials. So the second fluorescence quenching process between C-153 and PDI is speculated to be a photoinduced electron transfer (PET) from C-153 to PDI. To verify this speculation, the redox potentials of C-153 and PDI are measured and the results are listed in Table 4. The free energy changes ($\Delta G_{\text{ET}}^{\circ}$) of the intermolecular PET in different solvents are calculated following the Born equation [56,57]:

Table 4

Half-wave redox potentials (vs. SCE) of C-153 and PDI in CH_2Cl_2 .^a

Compounds	Oxd ₂	Oxd ₁	Red ₁	Red ₂	$\Delta E_{1/2}^{\circ}$ ^b
C-153	–	1.00	–0.73	–	0.87
PDI	1.78	1.28	–0.72	–0.95	2.00

^a Values obtained in dry CH_2Cl_2 with 0.1 M tetrabutylammonium phosphate (TBAP) as the supporting electrolyte.

^b $\Delta E_{1/2}^{\circ} = \text{Oxd}_1 - \text{Red}_1$.

$$\Delta G_{ET}^{\circ} = E_{ox} - E_{red} - Es - \frac{e^2}{4\pi\epsilon_0\epsilon_s r_{DA}} + \frac{e^2}{4\pi\epsilon_0} \left(\frac{1}{2r_D} + \frac{1}{2r_A} \right) \left(\frac{1}{\epsilon_s} - \frac{1}{\epsilon_{sp}} \right) \quad (4)$$

where E_{ox} and E_{red} are the oxidation potentials of C-153 and reduction potentials of PDI respectively. Es is the energy of the 0–0 transition of C-153 and r_{DA} represents the center to center distance between donor and acceptor, ϵ_0 is the absolute dielectric constant, ϵ_s is the dielectric constant of the solvents, and ϵ_{sp} is the dielectric constant of dichloromethane, in which the redox potentials of C-153 and PDI are measured. r_D and r_A are the ionic radii of C-153 and PDI respectively. The calculated ΔG_{ET}° for different solvents are all negative, therefore, the electron transfer from C-153 to PDI are thermodynamically favorable reactions. Moreover, the fluorescence quenching efficiency of C-153 by PDI increases significantly along with the polarity increase of the solvents. This is a typical characteristic of PET dominated fluorescence quenching process due to the polar solvent could accelerate the PET reaction by stabilizing the charge separated states [58,59]. Therefore, it can be conclude that the second fluorescence quenching process between C-153 and PDI is PET.

The PET efficiency (Φ_{ET}) between C-153 and PDI can be estimated from Eq. (5) based on the assumption that no other fluorescence quenching process present in the system except the energy and electron transfer.

$$\Phi_{ET} = \Phi_q - \Phi_{Ent} \quad (5)$$

The results are also summarized in Table 3. In the microemulsion, the electron transfer efficiencies are significantly larger than the energy transfer efficiencies, which indicate that the electron transfer dominating the fluorescence quenching process. However, in conventional organic solvents, such as THF and toluene, the energy transfer dominates the fluorescence quenching process. This result suggests that the environment in microemulsion favors the electron transfer process.

Stern–Volmer fluorescence quenching plots of C-153 in the presence of PDI at different concentrations in three solvents are shown in Fig. 7. The graphical analysis reveals that the fluorescence quenching process of C-153 by PDI in microemulsion is quite different from that in organic solvents. The linear Stern–Volmer plots in toluene and THF suggest pure dynamic quenching processes. The Stern–Volmer quenching constants (K_{SV}) calculated from the

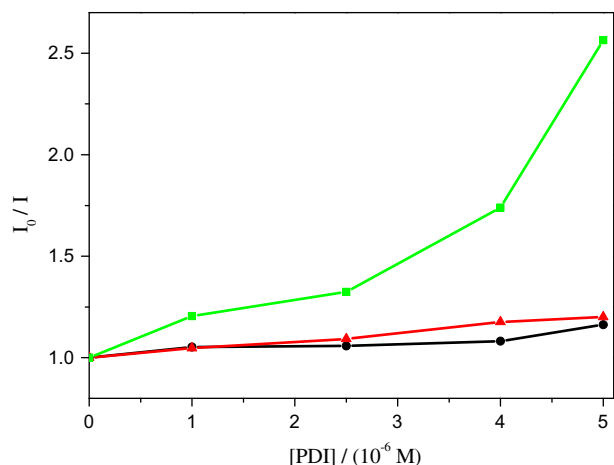


Fig. 7. Stern–Volmer plots of C-153 with quenching by PDI in toluene (black line), THF (red line), and microemulsion (green line). (For interpretation of the references to color in this figure legend, the reader is referred to the web version of this article.)

slop of the plots are $9.2 \times 10^5 \text{ M}^{-1}$ and $9.9 \times 10^5 \text{ M}^{-1}$, respectively, which are close to that found for a diffusion controlled fluorescence quenching process [60,61].

However, in the microemulsion, the Stern–Volmer plot shows an obvious upward curvature along with the PDI concentration increase. This non-linear Stern–Volmer plot suggests strongly the presence of static quenching mechanism between C-153 and PDI. As mentioned above, both C-153 and PDI stay at the interface between IL pool and TX-100, the local concentrations of both C-153 and PDI at the interface are much higher than that of bulky solution. Because of the high viscosity of TX-100 and IL, the diffusion of C-153 and PDI in microemulsion is extremely slow and the fluorescence quenching caused by dynamic collision between C-153 and PDI molecules is negligible. Due to the high local concentrations of both PDI and C-153 at the interface between TX-100 and IL pool, the probability of the PDI molecules present around the excited C-153 is large. Therefore, the static quenching dominates the fluorescence quenching process [62,63].

This static fluorescence quenching mechanism is also supported by the fluorescence lifetime measurements (see Figs. S5 and S6 in Supplementary material). Fluorescence lifetimes of C-153 and PDI in the microemulsion are measured to be 4.66 ns at 524 nm and 7.04 ns at 602 nm respectively. The 1:1 mixture of C-153 and PDI in the microemulsion presents fluorescence lifetime of 4.77 ns at 524 nm and 6.87 ns at 602 nm, which can be attributed to the emission of C-153 and PDI respectively. These measured fluorescence lifetimes for the 1:1 mixture are almost identical to those of C-153 or PDI alone in the microemulsion, which suggested again the static fluorescence quenching mechanism between C-153 and PDI, due to dynamic fluorescence quenching normally leads to significantly shortened fluorescence lifetime for the donor. Because the static fluorescence quenching is so quick and efficient in the microemulsion that the excited C-153 molecules which surrounded by PDI molecules do not contribute to the fluorescence at all, therefore, the measured fluorescence lifetime of C-153 in the 1:1 mixture is similar with that measured for C-153 alone in the microemulsion.

For a given donor–acceptor pair, the electron transfer rate is predominately determined by the donor–acceptor distance. Smaller donor–acceptor distance will benefit the electron transfer significantly. The static mechanisms for the fluorescence quenching of C-153 by PDI as revealed by Stern–Volmer fluorescence quenching plots and fluorescence lifetime measurements indicated that the donor–acceptor distance is small in the IL microemulsions. However, in organic solvents, the fluorescence quenching mechanisms is pure dynamic collision quenching process and the average distance between donor and acceptor is larger than that in the IL microemulsions. Therefore, the fluorescence quenching process in the IL microemulsion is dominated by electron transfer, while that in conventional organic solvent is dominated by energy transfer.

4. Conclusions

In summary, the amphiphilic PDI molecules adsorb at the interface between TX-100 and IL in these ternary IL microemulsions. The UV–vis and fluorescence spectra revealed that the fluorescence of C-153 was efficiently quenched by PDI. Photoinduced energy and electron transfer are found to be responsible for this fluorescence quenching. Compared with conventional organic solvents, such as THF and toluene, the IL microemulsions promote efficient fluorescence quenching by accelerating the electron transfer. Previous research revealed that an energy donor situated in a different region will transfer energy to the acceptor at a different rate [14]. Our results revealed that the competition between photoinduced energy and electron transfer can be tuned by the local environment

in microemulsions. All these results suggest that it is possible to achieve a full control over the electron or energy transfer by putting the donor or acceptor molecules in different regions of microemulsions. This is meaningful for the design and fabrication of artificial light harvesting systems or photosynthesis reaction centers. Further studies on the photoinduced energy or electron transfer in different microemulsion regions are now going on in our lab.

Acknowledgments

Financial support from the Natural Science Foundation of China (Grant Nos. 20771066 and 2064042467), Ministry of Education of China are gratefully acknowledged.

Appendix A. Supplementary material

Supplementary data associated with this article can be found, in the online version, at [doi:10.1016/j.jcis.2010.09.069](https://doi.org/10.1016/j.jcis.2010.09.069).

Reference

- [1] H.X. Gao, J.C. Li, B.X. Han, W.N. Chen, J.L. Zhang, R. Zhang, D.D. Yan, *Phys. Chem. Chem. Phys.* 6 (2004) 2914.
- [2] Y.A. Gao, S.B. Han, B.X. Han, G.Z. Li, D. Shen, Z.H. Li, J.M. Du, W.G. Hou, *Langmuir* 21 (2005) 5681.
- [3] D. Chakrabarty, D. Seth, A. Chakraborty, N. Sarkar, *J. Phys. Chem. B* 109 (2005) 5753.
- [4] D. Seth, A. Chakraborty, P. Setua, N. Sarkar, *Langmuir* 22 (2006) 7768.
- [5] N. Li, Y. Gao, L.Q. Zheng, J. Zhang, Y. Li, X.W. Li, *Langmuir* 23 (2007) 1091.
- [6] R. Schomäcker, K. Stickdorn, W. Knoche, *J. Chem. Soc., Faraday Trans.* 87 (1991) 847.
- [7] A.R. Elrington, Rapid Deactivation of Mustard in Microemulsion Technology, Ph.D. Thesis, Emory University, Atlanta, GA, 1990.
- [8] M. Spiro, D.M. de Jesus, *Langmuir* 16 (2000) 2464.
- [9] P. Lopez, A. Rodriguez, C. Gomez-Herrera, F. Sanchez, M.A. Moya, *J. Chem. Soc., Faraday Trans.* 88 (1992) 2701.
- [10] R.A. Mackay, *Adv. Colloid Interface Sci.* 15 (1981) 131.
- [11] S.G. Oh, J. Kizling, K. Holmberg, *Colloids Surf., A* 97 (1995) 169.
- [12] K. Holmberg, E. Österberg, *Prog. Colloid Polym. Sci.* 82 (1990) 181.
- [13] Y.L. Khmel'nitski, A.V. Kabanov, N.L. Klyachko, A.V. Levashov, K. Martinek, in: M.P. Pileni (Ed.), *Structure and Reactivity in Reversed Micelles*, Elsevier, Amsterdam, 1989.
- [14] A. Adhikari, D.K. Das, D.K. Sasmal, K. Bhattacharyya, *J. Phys. Chem. A* 113 (2009) 3737.
- [15] M.R. Wasielewski, *J. Org. Chem.* 71 (2006) 5051.
- [16] J.A.A.W. Elemans, R. van Hameren, R.J.M. Nolte, A.E. Rowan, *Adv. Mater.* 18 (2006) 1251.
- [17] K.Y. Law, *Chem. Rev.* 93 (1993) 449.
- [18] H. Langhal, *Helv. Chim. Acta* 88 (2005) 1309.
- [19] F. Würthner, *Chem. Commun.* (2004) 1564.
- [20] C.D. Dimitrakopoulos, P.R.L. Malenfant, *Adv. Mater.* 14 (2002) 99.
- [21] B.A. Jones, M.J. Ahrens, M.H. Yoon, A. Facchetti, T.J. Marks, M.R. Wasielewski, *Angew. Chem., Int. Ed.* 43 (2004) 6363.
- [22] F. Yukruk, A.L. Dogan, H. Canpinar, D. Guc, E.U. Akkaya, *Org. Lett.* 7 (2005) 2885.
- [23] Z. Chen, M.G. Debije, T. Debaerdemaeker, P. Osswald, F. Würthner, *ChemPhysChem* 5 (2004) 137.
- [24] P. Jonkheijm, N. Stutzmann, Z. Chen, D.M.E. de Leeuw, W. Meijer, A.P.H.J. Schenning, F. Würthner, *J. Am. Chem. Soc.* 128 (2006) 9535.
- [25] P.R.L. Malenfant, C.D. Dimitrakopoulos, J.D. Gelorme, L.L. Kosbar, T.O. Graham, *Appl. Phys. Lett.* 80 (2002) 2157.
- [26] B.A. Gregg, R.A. Cormier, *J. Am. Chem. Soc.* 123 (2001) 7959.
- [27] A.J. Breeze, A. Salomon, D.S. Ginley, B.A. Gregg, H. Tillmann, H.H. Horhold, *Appl. Phys. Lett.* 81 (2002) 3085.
- [28] B.A. Gregg, *J. Phys. Chem.* 100 (1996) 852.
- [29] C.C. You, C.R. Saha-Mler, F. Würthner, *Chem. Commun.* (2004) 2030.
- [30] J. Hua, F. Meng, F. Ding, F. Li, H. Tian, J. Mater. Chem. 14 (2004) 1849.
- [31] E.E. Neuteboom, P.A. van Hal, R.A.J. Janssen, *Chem. Eur. J.* 10 (2004) 3907.
- [32] M.A. Angadi, D. Gosztola, M.R. Wasielewski, *Mater. Sci. Eng., B* 63 (1999) 191.
- [33] P. Ranke, I. Bleyl, J. Simmerer, D. Haarer, A. Bacher, H.W. Schmidt, *Appl. Phys. Lett.* 71 (1997) 1332.
- [34] S. Alibert-Fouet, S. Dardel, H. Bock, M. Oukachmih, S. Archambeau, I. Seguy, P. Jolinat, P. Destruel, *ChemPhysChem* 4 (2003) 983.
- [35] P. Schouwink, A.H. Schafer, C. Seidel, H. Fuchs, *Thin Solid Films* 372 (2000) 163.
- [36] T. Zukawa, S. Naka, H. Okada, H. Onnagawa, *J. Appl. Phys.* 91 (2002) 1171.
- [37] L. Fleury, A. Zumbusch, M. Orrit, R. Brown, J. Bernard, *J. Lumin.* 56 (1993) 15.
- [38] W.E. Moener, T. Plakhotnik, T. Irgartinger, M. Croci, V. Palm, U.P. Wild, *J. Phys. Chem.* 98 (1994) 7382.
- [39] S. Kummer, T. Basche, C. Brauchle, *Chem. Phys. Lett.* 229 (1994) 309.
- [40] T. Basche, S. Kummer, C. Brauchle, *Nature* 373 (1995) 132.
- [41] F. Kulzer, S. Kummer, R. Matzke, C. Brauchle, T. Basche, *Nature* 387 (1997) 688.
- [42] P. Schlichting, B. Duchscherer, G. Seisenberger, T. Basche, C. Brauchle, K. Mullen, *Chem. Eur. J.* 5 (1999) 388.
- [43] K.D. Belfield, K.J. Schafer Jr., M.D. Alexander, *Chem. Mater.* 12 (2000) 1184.
- [44] T. Ishi-I, K. Murakami, Y. Imai, S. Mataka, *Org. Lett.* 7 (2005) 3175.
- [45] T. van der Boom, R.T. Hayes, Y. Zhao, P.J. Bushard, E.A. Weiss, M.R. Wasielewski, *J. Am. Chem. Soc.* 124 (2002) 9582.
- [46] M.J. Ahrens, L.E. Sinks, E. Rybtchinski, W.H. Liu, B.A. Jones, J.M. Giaimo, A.V. Gusev, A.J. Goshe, D.M. Tiede, M.R. Wasielewski, *J. Am. Chem. Soc.* 126 (2004) 8284.
- [47] X.Y. Li, L.E. Sinks, B. Rybtchinski, M.R. Wasielewski, *J. Am. Chem. Soc.* 126 (2004) 10810.
- [48] J. Dupont, C.S. Consorti, P.A.Z. Suarez, R.F. Souza, *Org. Synth.* 79 (1999) 236.
- [49] G. Gritzner, *Pure Appl. Chem.* 62 (1990) 1839.
- [50] A. Adhikari, K. Sahu, S. Dey, S. Ghosh, U. Mandal, K. Bhattacharyya, *J. Phys. Chem. B* 111 (2007) 12809.
- [51] D.M. Zhu, X. Wu, Z.A. Schelly, *J. Phys. Chem.* 96 (1992) 7121.
- [52] We can not find an excitation wavelength to exclusively excited C-153 because of the overlap of the absorption spectra of C-153 with that of PDI.
- [53] R.S. Loewe, K.Y. Tomizaki, W.J. Youngblood, Z. Bo, J.S. Lindsey, *J. Mater. Chem.* 12 (2002) 3438.
- [54] K. Muthukumar, J.K. Schwartz, I.V. Sazanovich, C. Kirmaier, E. Hindin, J.R. Diers, M. Taniguchi, D.F. Bocian, D. Holten, J.S. Lindsey, *J. Phys. Chem. B* 107 (2003) 3443.
- [55] S. Xiao, M.E. El-Khouly, Y. Li, Z. Gan, H. Liu, L. Jiang, Y. Araki, O. Ito, D. Zhu, *J. Phys. Chem. B* 109 (2005) 3658.
- [56] R.F. Kelley, W.S. Shin, B. Rybtchinski, L.E. Sinks, M.R. Wasielewski, *J. Am. Chem. Soc.* 129 (2007) 3173.
- [57] A.Z. Weller, *Phys. Chem. N. F.* 133 (1982) 93.
- [58] G.L. Closs, J.R. Miller, *Science* 240 (1988) 440.
- [59] W. Xu, H.L. Chen, Y.F. Wang, C.T. Zhao, X.Y. Li, S.Q. Wang, Y.X. Weng, *ChemPhysChem* 9 (2008) 1409.
- [60] S. Lis, *J. Alloys Compd.* 341 (2002) 45.
- [61] S.C.J. Meskers, H.P.J.M. Dekkers, *J. Phys. Chem. A* 105 (2001) 4589.
- [62] H.C. Komaromy, N. Calkins, R. von Wandruszka, *Langmuir* 12 (1996) 916.
- [63] M.R. Eftink, C.A. Ghiron, *J. Phys. Chem.* 80 (1976) 486.